Journal of Power Sources 198 (2012) 408–415

Contents lists available at SciVerse ScienceDirect

Journal of Power Sources

journal homepage: www.elsevier.com/locate/jpowsour

Effects of electrolyte composition on the electrochemical activation of alkali-treated soft carbon as an electric double-layer capacitor electrode

Tomoki Ohta, In-Tae Kim, Minato Egashira, Nobuko Yoshimoto, Masayuki Morita*

Graduate School of Science and Engineering, Yamaguchi University 2-16-1, Tokiwadai, Ube, 755-8611, Japan

ARTICLE INFO

Article history:
Received 8 August 2011
Received in revised form 2 October 2011
Accepted 3 October 2011
Available online 8 October 2011

Keywords:
Electric double-layer capacitor
Alkali-treated soft carbon
Electrochemical activation
Electrolyte composition
Ion-insertion

ABSTRACT

The electrochemical behavior of alkali-treated soft carbon (ASC) has been investigated in organic electrolyte solutions with different compositions. So-called electrochemical activation phenomena, in which higher capacitive currents are observed after certain anodic or cathodic polarization in the electrolyte solutions, depended on the electrolyte composition as well as its polarization condition. The anodic polarization in tetraethylammonium tetrafuruoroborate ($TEABF_4$) solutions induced higher capacitive currents in the positive potential region where the electrochemical adsorption/desorption of anion acts as a charge compensation process, while the activation by cathodic polarization in $TEABF_4$ solutions increased the capacitive currents associated with the cation adsorption/desorption. The electrolyte solvent also affected the activation process, especially for the cathodic activation. Larger sizes of ions and solvent molecules were generally effective for the activation, while the smaller sizes of them were preferable to obtain higher capacitance for the resulting electrochemically activated carbon.

1. Introduction

Electrochemical capacitors (ECCs) are efficient energy storage devices that have wide applications from small size memory back-up uses to power assistance for electric vehicles (EVs) because of their high power density and long cycle life [1–3]. However, the energy densities of ECCs are generally much lower than those of rechargeable batteries. Among ECCs, electric double-layer capacitor (EDLC) has excellent cycle life but limited capacitance compared by other types of ECCs that utilize pseudo-capacitance based on Faradaic reactions. Thus, the improvement of the electrostatic capacitance has been the major aim in developing advanced EDLCs.

In general, activated carbon (AC) with high specific surface area (500–2000 $m^2\,g^{-1}$) has been used as both positive and negative electrodes in EDLC [4–6]. This type of carbon materials inevitably restricts the volumetric specific capacitance of the resulting EDLC to less than 20 $F\,cm^{-3}$, due to relatively low density of such high surface area carbon materials [7,8]. Recently, so-called hybrid electrochemical capacitors (HECs) that utilize a Faradaic reaction of battery electrode (e.g. graphite), typically as the negative electrode, has attracted much attention because of their higher energy density than that of conventional EDLC and of higher power density than that of lithium-ion battery (LIB) [9–11]. For example, a combination of graphite negative electrode and activated carbon positive electrode has both higher specific capacity and higher operation voltage than those of conventional EDLC, which results in higher energy density of the capacitor device. As the positive electrode for such HECs using graphite-based negative electrodes, higher specific capacity as well as higher operation potential is required.

Takeuchi et al. first reported a high energy density EDLC using non-porous graphitizable carbon (so-called soft-carbon) pre-treated with alkali (KOH) [12,13]. They found an activation phenomenon for the soft-carbon, i.e. the electrostatic capacitance being significantly increased after electrochemical polarization. They called it "Electric-field Activation". In spite of larger particle size (>10 μm) and smaller specific surface area (<100 $m^2\,g^{-1}$) than those of activated carbon particles, some of soft carbons from calcined aromatic resins showed higher specific capacitance than commercially available activated carbon [12–15]. With respect to the activation mechanism of such carbon materials, Takeuchi et al. [12,13] and Kim et al. [15] suggest that insertion or intercalation of ions and solvent molecules into the narrow space inside the carbon material would occur at the first polarization, and hence additional active sites for ion adsorption would evolved.

Aida et al. also observed a similar electrochemical activation phenomenon for alkali-treated soft carbon (ASC), and showed that it is applicable to the positive electrode of an HEC with a combination of hard carbon (HC) as the negative electrode [16]. The resulting HC/ASC capacitor, called "advanced HEC", has much higher power and energy densities than those of conventional EDLC, mainly due to its high operation voltage. However, the details of the activation processes of ASC itself have not been fully understood.

* Corresponding author. Tel.: +81 836 85 9211; fax: +81 836 85 9201.
E-mail address: morita@yamaguchi-u.ac.jp (M. Morita).

0378-7753/$ – see front matter © 2011 Elsevier B.V. All rights reserved.
doi:10.1016/j.jpowsour.2011.10.006

We have been interested in the influences of the electrolyte composition on the electric double-layer capacitance of different carbon materials [17–19]. It has been concluded that not only the ionic species but also the solvent of the electrolyte significantly affect the capacitance behavior of carbon electrodes. Thus, in this work, we have investigated the effects of the electrolyte composition on the electrochemical activation of ASC. The capacitance behavior of an ASC electrode has been examined before and after the electrochemical polarization using different combinations of electrolytic salt and organic solvent. Changes in the voltammetric response during the anodic and cathodic polarization were monitored as a function of the electrolytic salt. Structure changes of ASC by the electrochemical activation were also investigated by XRD experiments. The capacitance behavior of the resulting activated ASC was evaluated by potential scanning voltammetry and constant-current charge–discharge measurements. Rate capability of the activated electrode is also discussed in connection with the mechanistic aspect of ASC in detail.

2. Experimental

2.1. Preparation of electrode and electrolyte solutions

The ASC sample was prepared from aromatic resin in a laboratory scale at Daihatsu Motor Co., Ltd. [16], which was further treated by heating in a vacuum oven at 200 °C for 1 h to remove impurities before use. The carbon material was mixed with carbon black as a conducting support and poly(tetrafluoroethylene) (PTFE) resin as a binder by 85:5:10 in mass ratio. Then, the mixture was pressed by a roller press to form a sheet with constant thickness (average mass: 5 mg for a sheet with 7 mm diameter). The resulting sheet was heated in a vacuum oven at 120 °C for 12 h, and then pressed at 100 kg cm^{-2} to form a disk electrode on a current collector of stainless steel mesh.

Acetonitrile (AN), propylene carbonate (PC), γ-butyrolactone (GBL), and a mixture of ethylene carbonate and dimethyl carbonate (EC+DMC, 1:1 in volume) were used as the organic solvents for electrolyte solutions. These were Battery Grade (Kishida Chemical) or Special Grade (Tomiyama Pure Chemical) reagents, and used as received without further purification. The electrolytic salts were lithium hexafluorophosphate ($LiPF_6$), lithium tetrafluoroborate ($LiBF_4$), tetraethylammonium tetrafluoroborate ($TEABF_4$), and 1-ethyl-3-methylimidazolium tetrafluoroborate ($EMIBF_4$), which were dissolved in the organic solvents with 1.0 mol dm^{-3} (M) concentration under a dry Ar atmosphere.

2.2. Electrochemical activation and evaluation of capacitor performances

All electrochemical measurements were carried out using a 3-electrode cell system. A Pt-sheet with high surface area and Ag wire in the same electrolyte solution were used as the counter and quasi-reference electrodes (QRE), respectively. The electrochemical activation was carried out by potential scanning with 2.0 mV s^{-1} using a conventional potentiostat (Hokuto Denko, HZ-3000) coupled with a personal computer. The potential limits for anodic and cathodic polarization were properly chosen depending on the electrolyte composition. After the electrochemical activation, the capacitor performance of the activated ASC electrode was evaluated in the same electrolyte composition by cyclic voltammetry (CV) in the potential range between 0.0 and 1.0 V with scan rate of 2 mV s^{-1}. In some case, the capacitor performances were evaluated after changing the electrolyte solution from that used for electrochemical activation. The constant current charge–discharge cycling was also carried out in the same potential range as in CV experiments (0.0–1.0 V) under different current densities (0.2–5.0 mA cm^{-2}) using a charge–discharge cycle tester (Nagano, BTS 2004).

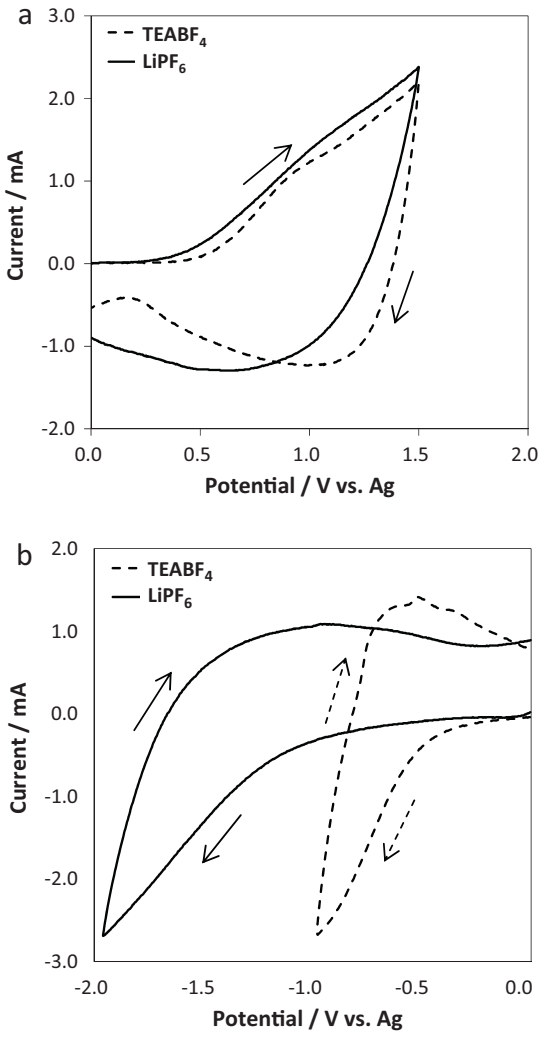

Fig. 1. Potential scanning voltammograms of ASC in EC+DMC (1:1 by volume) solutions containing 1.0 M $TEABF_4$ or 1.0 M $LiPF_6$, during (a) positive polarization and (b) negative polarization, with potential scanning rate of 2 mV s^{-1}.

After the electrochemical activation in 1.0 M $LiPF_6$ with different electrolyte solvents, the CV response in 1.0 M $LiPF_6$/EC+DMC was also recorded in the potential range between −2.0 and 1.5 V. These experiments were done for examining the influences of the electrolyte solvent for electrochemical activation on the capacitor performance of the resulting electrodes.

Structure changes of the carbon material during the electrochemical activation were examined by *ex-situ* X-ray diffraction (XRD) analysis. In this experiment, the ASC electrode was activated at constant-potential polarization in the electrolyte with different compositions. The activated electrodes were rinsed thoroughly with the organic solvent examined and then set to a conventional diffractometer (Shimadzu, XD-D1, CuKα radiation).

3. Results and discussion

3.1. Influences of electrolyte composition on the electrochemical activation

Typical current responses of a flesh ASC electrode during the first cycle of potential scanning in electrolyte solutions with EC+DMC solvent are shown in Fig. 1. The on-set potential where the current

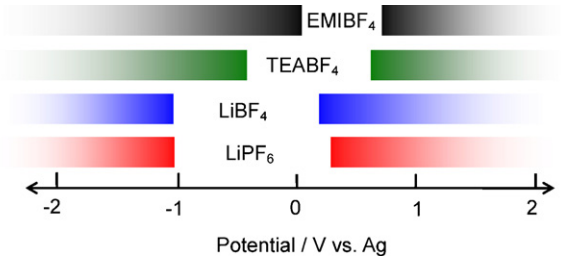

Fig. 2. Summary of onset potential for the electrochemical activation in EC+DMC dissolving different electrolytic salts, the data was obtain by potential scanning voltammograms (2 mV s^{-1}).

increases steeply was around 0.4 V vs. Ag QRE for anodic polarization, regardless of the electrolytic salt (Fig. 1a). On the other hand, the on-set potential for cathodic current increase depended on the electrolytic salt, as shown in Fig. 1b. It has been generally accepted that the anionic and cationic species in the electrolytes would respectively take part in the electrochemical activation by the anodic and the cathodic polarization [12,13,15]. Thus, there would be no intrinsic difference between BF_4^- and PF_6^- anions in the activation process during the anodic polarization. However, the clear difference in the on-set potential for the cathodic polarization suggests that the activation process depends much on the cation species, Li^+ and TEA^+.

Fig. 2 summarizes the on-set potential, at which the current increases steeply, for the electrochemical activation of ASC in the EC+DMC solution dissolving different electrolytic salts. The bars in the figure indicate potential regions where the activation occurs. The on-set potential for cathodic polarization in $LiBF_4$ solution was around −1.0 V, which was almost the same in the case using $LiPF_6$ salt. The on-set potential in the solution containing $EMIBF_4$ was apparently higher than that in $TEABF_4$. These differences in the on-set potential among the cation species strongly suggest that the cation of the salt can participate in the cathodic activation process. On the other hand, the on-set potential for the anodic polarization depended not only on the anion but also cation species. The differences in the anodic on-set potentials among the salts with the same anion ($LiBF_4$, $TEABF_4$ and $EMIBF_4$) seem to relate with the potential of zero-charge (PZC) of the carbon electrode. The PZC at glassy carbon electrode was found to be dependent much on the cation in the electrolyte [18]. That is, the order of the PZC value, $LiBF_4 \sim LiPF_6 < TEABF_4 < EMIBF_4$, was qualitatively consistent with that of the anodic on-set potential. These findings reveal that not only the chemistry of charged species but also the strength of the electrochemical overvoltage, or electrostatic field at the electrode/electrolyte interface, would cause the electrochemical activation of ASC.

In order to simplify the discussion, we would hereafter show the selected experimental results for the electrolyte solutions of $LiPF_6$ and $TEABF_4$ as the representatives of different salts. In Fig. 3, capacitive current responses of ASC electrode after the electrochemical activation are summarized, where AN-based solutions dissolving different electrolytic salts are employed and the current response in each fifth cycle is recorded as the steady-state response. Even after the same activation condition, anodically polarized in the potential range between 0.0 and 1.5 V, different current responses were observed for the solutions containing $TEABF_4$ and $LiPF_6$, especially in the potential range below 0.5 V (Fig. 3a). Here, the observed current responses should be non-Faradaic because possible Faradaic processes accompanied by the electrochemical activation had been completed before this measurement. According to experimental data on apparent potential of zero charge (PZC) of carbon-based electrode in organic electrolyte solutions [18,19], the charge compensation process of the present ASC electrode should be anion

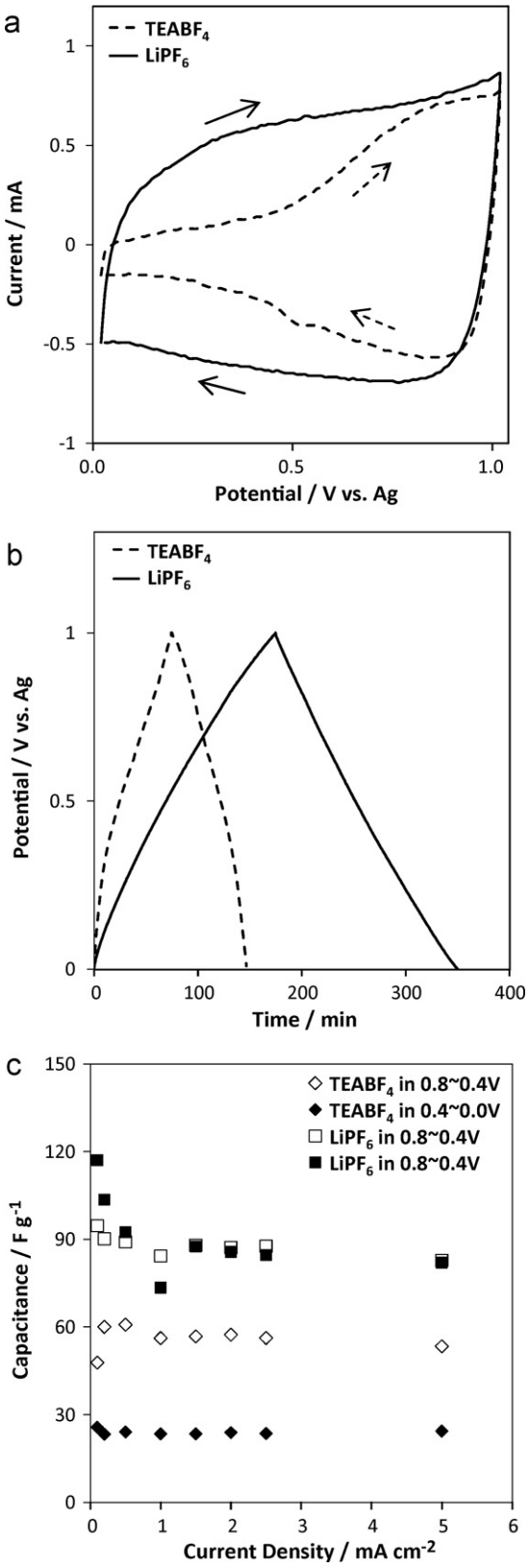

Fig. 3. (a) Cyclic voltammograms (2 mV s^{-1}), (b) constant-current polarization (0.2 mA cm^{-2}), and (c) rate capability of discharge capacitance on ASC in AN solutions containing 1.0 M $TEABF_4$ or 1.0 M $LiPF_6$, after the activation with positive polarization (0.0–1.5 V vs. Ag QRE) in the same electrolyte solution.

adsorption in the potential region above 0.5 V, and the cation adsorption below 0.4 V. The current response shown in Fig. 3a strongly suggests that the activation in the $TEABF_4$ solution with anodic polarization (from 0.0 to 1.5 V) is not effective for cation (TEA^+) adsorption at the resulting ASC. On the other hand, the anodic activation in $LiPF_6$ will be effective for the cation (Li^+) adsorption after the activation.

The potential profiles during the constant-current charge–discharge cycling (Fig. 3b; 0.2 mA cm^{-2}) also support above discussion. The slope of potential–time curve for the electrode activated and measured in the $TEABF_4$ solution changes at around 0.5 V, which indicates the charge compensation process also changes at this potential. The charge and discharge capacitances of ASC are determined from the slopes of the linear parts in the potential–time curves shown in Fig. 3b. The resulting value of discharge branch for each potential region (0.0–0.4 V, and 0.4–0.8 V) is plotted as a function of the current density in Fig. 3c. As expected from the potential profiles in Fig. 3b, the discharge capacitance in the $TEABF_4$ solution was much lower in the potential range of 0.0–0.4 V than that observed in the potential range above 0.4 V. On the other hand, the discharge capacitance determined in the $LiPF_6$ solution did not change with the potential region examined. In both electrolyte systems, the rate (current density) dependence of the discharge capacitance was rather small, except for the case with very low current density. This result suggests that, if the charge compensation process consists of simple adsorption/desorption of ions at the electrode/electrolyte interface, the geometry of the active site for ion-adsorption will be simple structure without complicated fine porosities.

Fig. 4 shows the results after the electrochemical activation with the polarization range between −1.0 and 1.5 V, where the electrode was activated both anodically and cathodically. The voltammetric responses after the activation (Fig. 4a) showed little difference between $TEABF_4$ and $LiPF_6$, which contrasts clearly with the result shown in Fig. 3a. That is, the cathodic activation (down to −1.0 V) in the $TEABF_4$ solution induces the active site for cation (TEA^+) adsorption in the ASC electrode. On the other hand, according to the results shown in Fig. 1b, contribution of Li^+ species to the cathodic activation will not be significant when the cathodic polarization is limited to −1.0 V, and more negative potential should be needed for the activation. Thus, the anodic activation with the contribution of PF_6^- anion will be enough to compensate the double-layer charge with Li^+ (or solvated Li^+) adsorption/desorption in the potential region below 0.4 V in Fig. 4a.

The potential profiles under the constant-current charge–discharge cycling (Fig. 4b; 0.2 mA cm^{-2}) reveal smaller differences in the slope of the linear part (capacitances) for operation potential ranges of 0.0–0.4 V and 0.4–0.8 V. In Fig. 4c, the rate capabilities of discharge capacitance under the constant-current cycling are summarized for different electrolyte solutions and different potential ranges. Although the capacitance value in $TEABF_4$ was generally smaller than that in $LiPF_6$, the difference in the operation voltage range (0.0–0.4 V and 0.4–0.8 V) influenced little on the discharge capacitance in each electrolyte.

Above experimental results prove that not only the electrolyte composition but also the polarization conditions participate in the electrochemical activation process at ASC, as already discussed in the previous part in this article. The influences of ionic species and the polarization conditions on the activation process are schematically illustrated in Fig. 5. Here the ionic radii in AN are: TEA^+ (0.34 nm) < Li^+ (0.45 nm, solvated) for cations, and BF_4^- (0.22 nm) < PF_6^- (0.33 nm) for anions [12,18,20,21]. When the ASC electrode is anodized in $TEABF_4$ solution, BF_4^- anion contributes to the evolution of active sites for ion-adsorption, whose geometry would fit to BF_4^- anion adsorption but will not be enough to adsorb the larger size of cation (TEA^+) (Fig. 5a). The anodization

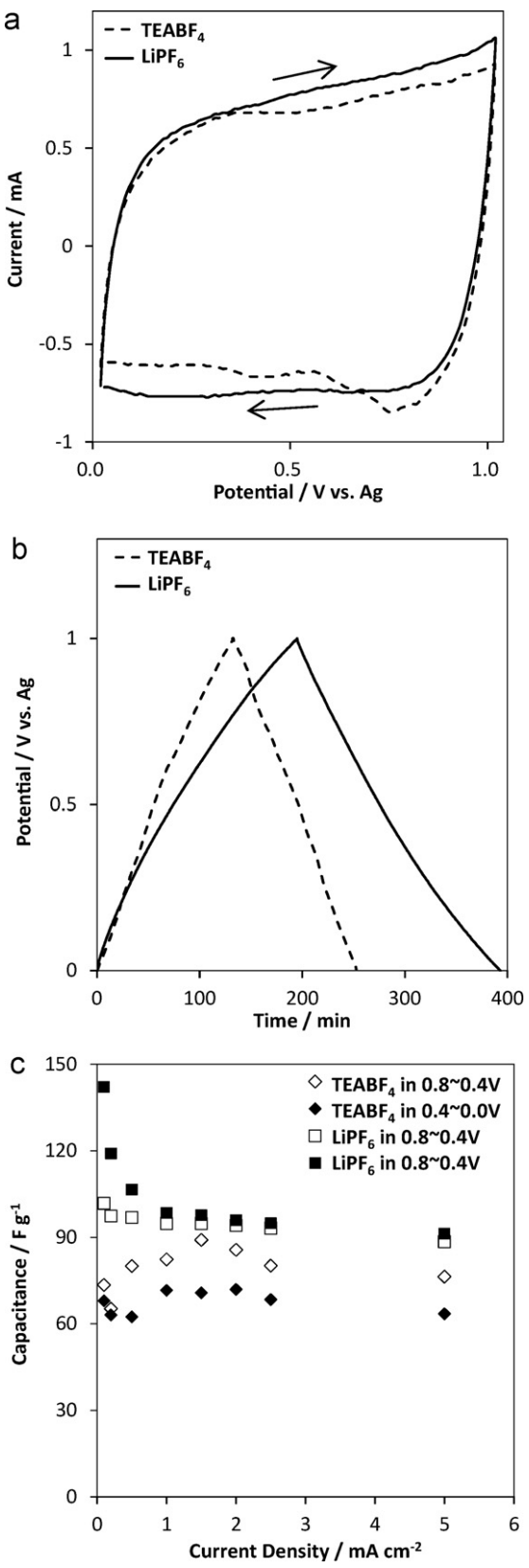

Fig. 4. (a) Cyclic voltammograms (2 mV s^{-1}), (b) constant-current polarization (0.2 mA cm^{-2}), and (c) rate capability of discharge capacitance on ASC in AN solutions containing 1.0 M $TEABF_4$ or 1.0 M $LiPF_6$, after the activation with positive and negative polarization (−1.5 to 1.5 V vs. Ag QRE) in the same electrolyte solutions.

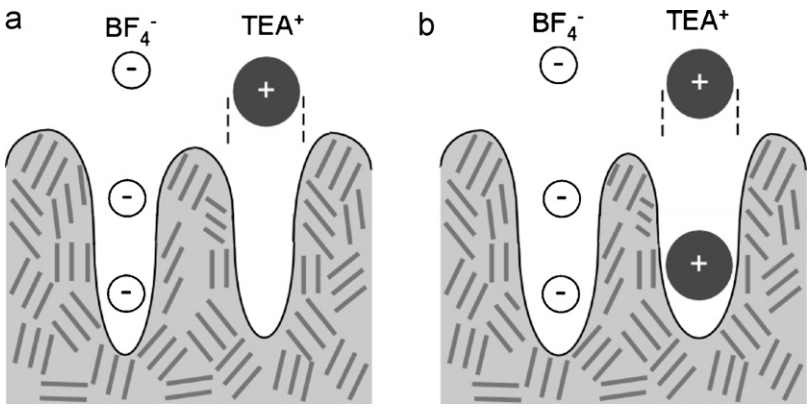

Fig. 5. Schematic diagram of the electrochemical activation of ASC and its capacitance evolution in $TEABF_4$ solutions, (a) activation with positive polarization followed by the capacitance measurement in $TEABF_4$ solution, and (b) activation with negative polarization followed by the capacitance measurement in $TEABF_4$ solution. Possible contribution of the solvent molecule to the capacitance evolution is not taken into account.

of ASC in the $LiPF_6$ solution would form new active sites for ion adsorption with wider space of pore structure because of larger size of PF_6^-. Such a newly developed pore structure will contribute to not only anion (PF_6^-) but also cation (solvated Li^+) adsorption/desorption. Here, the size of solvated Li^+ in bulk solution is larger than that of PF_6^-, but some partial de-solvation would be enable itself to be transported in the pore structure. On the other hand, the activation by the cathodic polarization, where the cation would take part in the process, would induce wider space for ion adsorption/desorption in ASC because of larger sizes of cations than those of anions.

The voltammetric responses of the ASC electrode in $LiPF_6$ solutions with different organic solvents are compared, after the electrochemical activation was done in each electrolyte composition. Fig. 6a shows the comparison of the steady-state current responses (5th cycle) after the activation. The electrolyte solvent influences much on the voltammetric response of ASC. The highest current (still non-Faradaic) was observed in $LiPF_6$/AN and the lowest in the PC solution among the electrolytes examined. In this result, certain effects of the solution viscosity, AN < GBL ~ EC+DMC < PC, would be included in part. Thus, the current response was compared in a common electrolyte system after the activation done in the electrolytes with different solvents. That is, the test electrodes activated in the solutions of different compositions were transferred to the cell containing a common electrolyte composition (e.g. $LiPF_6$/EC+DMC) and then the capacitive current response was measured. Typical results are summarized in Fig. 6b, where $LiPF_6$/EC+DMC was employed as the electrolyte system for capacitance evaluation. Three electrodes activated in EC+DMC, GBL and PC showed almost the same current response when examined in the same electrolyte composition of $LiPF_6$/EC+DMC. On the other hand, the ASC electrode activated in AN showed smaller current response than those activated in the other solvent systems. This seems to be inconsistent with the result shown in Fig. 6a, where the activation in the AN-based electrolyte showed the highest current response. However, this apparent inconsistency can be explained by the possible contribution of the solvent molecule to the activation process. When the activation is done in the solution with smaller size of solvent molecule (i.e. AN), high capacitive current can be achieved in the same (AN) electrolyte solution, but smaller current responses will be observed in the solution consisting of larger size of solvent molecule (e.g. EC+DMC). This argument is schematically shown in Fig. 7. In this context, we could conclude that the solvent molecule affects the activation process much. The molecular size as well as such properties as wettability and viscosity of the solvent can contribute to the activation process of ASC.

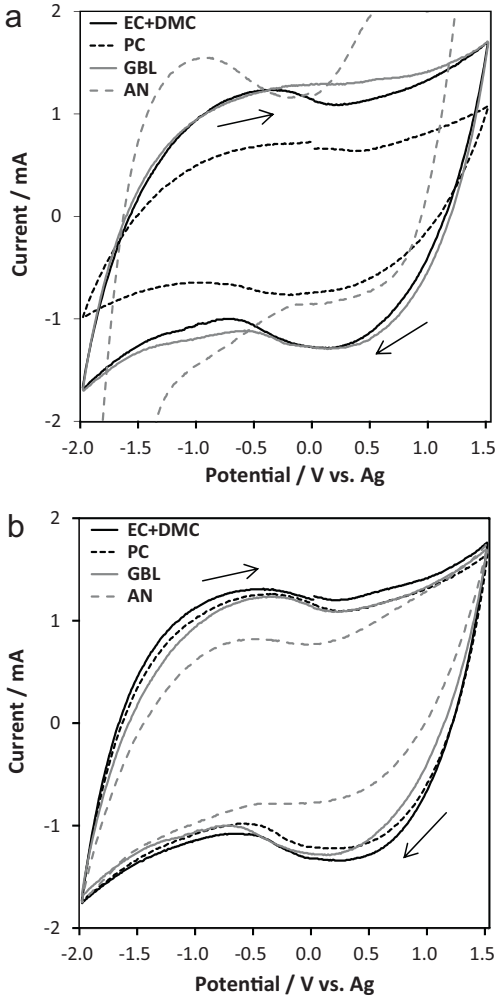

Fig. 6. Cyclic voltammograms ($2\,mV\,s^{-1}$) of ASC (a) activated and measured in various organic solvent solutions containing 1.0 M $LiPF_6$, and (b) activated in various organic solvent solutions containing 1.0 M $LiPF_6$ and measured in 1.0 M $LiPF_6$/EC+DMC.

3.2. Analysis of the activation condition

Fig. 8 shows *ex-situ* XRD patterns of the ASC electrode before, during and after the electrochemical activation. Each diffraction pattern corresponds to that for the sample treated at the potential

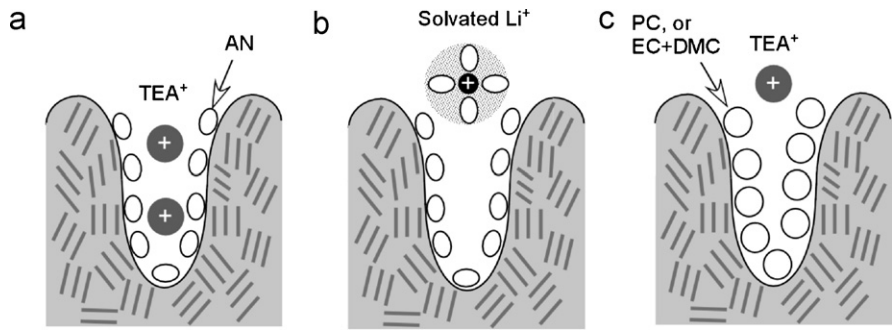

Fig. 7. Schematic diagram of the capacitance evolution for ASC that was beforehand activated in $TEABF_4$/AN, for the cases of (a) the capacitance evolution with TEA^+ in AN, (b) the capacitance evolution with Li^+ in AN, and (c) the capacitance evolution with TEA+ in carbonates (PC, EC+DMC).

of the CV curve in the insert. The ACS sample before the activation (A) has a broad diffraction peak at around $2\theta \sim 24^\circ$, which indicates that the average structure involves stacks of graphene layers with a long-range disordered structure (average *d*-spacing ~0.37 nm). Simple immersion of ASC in the electrolytic solution of $LiPF_6$/EC+DMC (B) does not change the diffraction pattern at all. However, the cathodic polarization in $LiPF_6$/EC+DMC induced the average structure changing little bit to those having lower 2θ values (C, D). The anodic polarization after the cathodization caused further changes in average *d*-spacing toward larger one (lower 2θ) (E, F). These changes in average *d*-spacing was somewhat reversible because the diffraction pattern of the ASC sample after the cycle (stopped at the initial rest potential) showed very small change, comparing with that of the original one. On the other hand, the potentiostatic polarization in $TEABF_4$/EC+DMC at −1.4 V also showed the shift of diffraction peak to lower angle (H). These results strongly suggest that a kind of ion-insertion takes place during the cathodic and anodic polarization for the electrochemical activation of ASC, and that the process would be partly reversible. Also this is well consistent with the fact that the ionic species strongly affect the activation process, as shown in the previous part of this work.

Based on the above discussion, we have examined an optimum combination of the electrochemical activation and the capacitance evaluation conditions. Fig. 9 shows the results for the case using $TEABF_4$/AN as the electrolyte for capacitance evaluation of ASC activated in different electrolyte compositions ($LiPF_6$/EC+DMC, $LiPF_6$/AN, and $TEABF_4$/AN). Here, the ASC electrode was activated by potential scanning with the potential range of −2.0 to 1.5 V in each electrolyte solution. The influence of the electrolyte composition used in the activation process was rather small, but the electrode treated in the same electrolyte composition as that used in the capacitance evaluation, $TEABF_4$/AN, gave the highest voltammetric current (Fig. 9a). The constant-current charge–discharge cycling (Figs. 9b; 2.0 mA cm^{-2} and c) also showed that the activation in $TEABF_4$/AN would lead to the highest capacitance for the capacitance evaluation in this electrolyte composition. Here, in Fig. 9b, the specific capacity (C g^{-1}), instead of time (min), is used as the abscissa in order to compare the specific capacitance of each electrode directly. As shown in Fig. 9c, for every case, we confirmed that the rate dependence is rather small up to the current density of 5 mA cm^{-2} (corresponding to ca."10 C rate").

Above results seem to be inconsistent with the previous one (e.g. in Fig. 4). It is noticeable that the optimized electrolyte composition for the present ASC material could depend on the electrolyte composition for capacitance evaluation. For example, larger sizes of ions (solvated Li^+ and PF_6^-) are necessary to activate ASC that would be used in a capacitor with electrolytes consisting of large sizes of ions. However, when smaller sizes of ions (TEA^+ and BF_4^-)

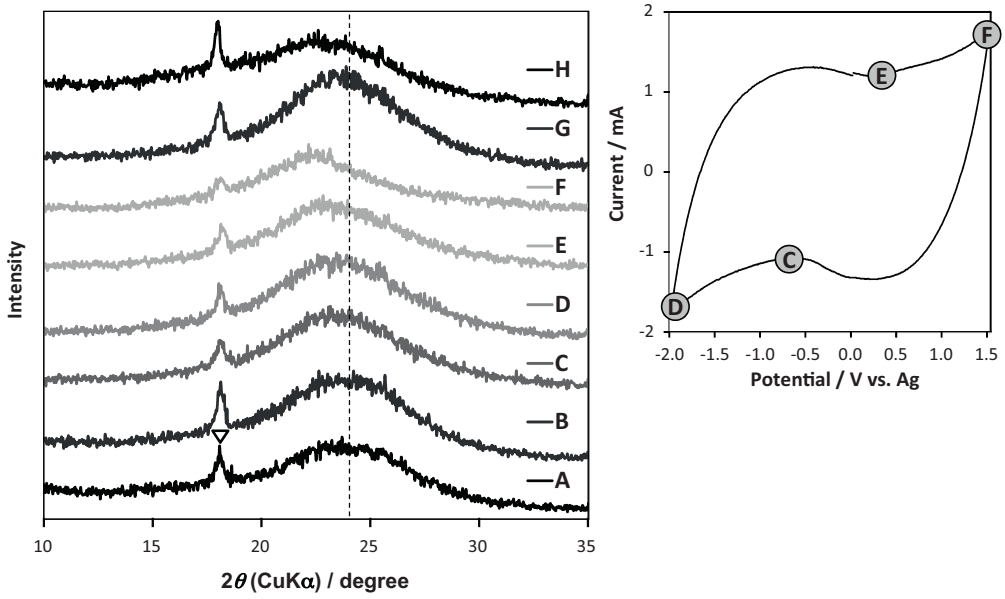

Fig. 8. XRD patterns of ASC before, during and after the electrochemical activation, A: before activation, B: after immersion in 1.0 M $LiPF_6$/EC+DMC, C: polarized at −0.7 V, D: polarized at −2.0 V, E: polarized at 0.5 V, F: polarized at 1.5 V, G: after CV measurement in $LiPF_6$/EC+DMC, H: polarized at −1.4 V in $TEABF_4$/EC+DMC (▽on each pattern indicates diffraction from PTFE binder in the electrode).

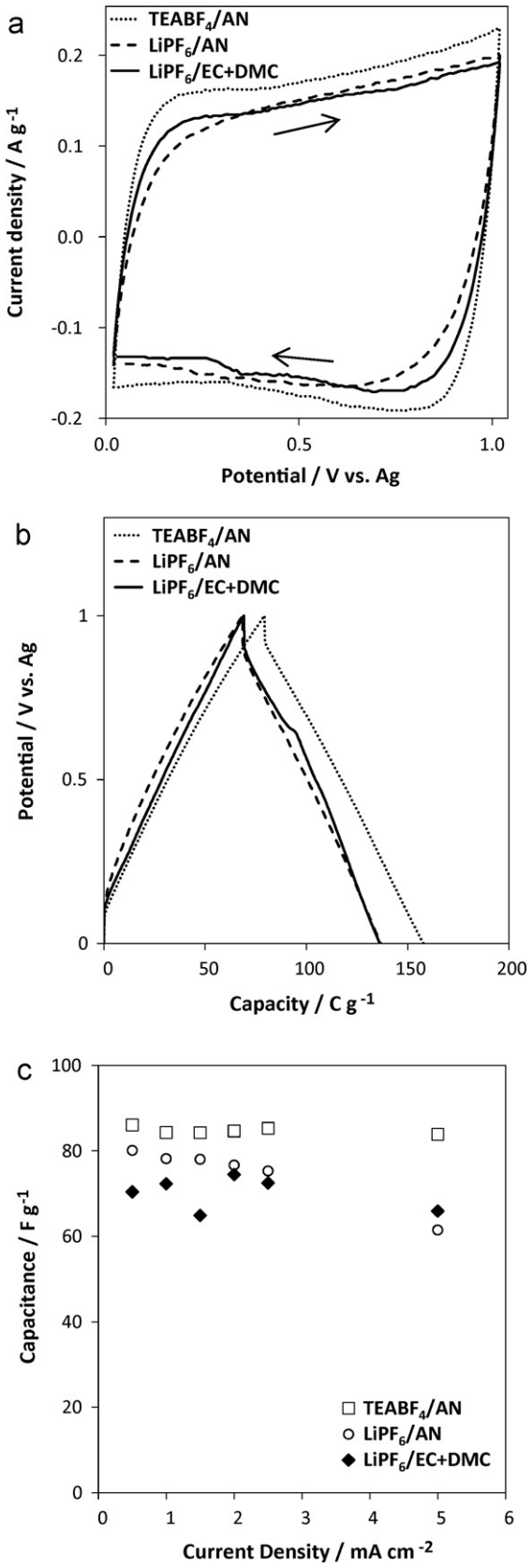

Fig. 9. (a) Cyclic voltammograms ($2\,mV\,s^{-1}$), (b) constant-current polarization ($2.0\,mA\,cm^{-2}$), and (c) rate capability of discharge capacitance on ASC measure in AN solution containing 1.0 M $TEABF_4$, after the activation with positive and negative polarization (−2.0 to 1.5 V vs. Ag QRE) in the electrolyte solutions with various compositions.

are used in the resulting capacitor, such larger sizes of ions would not be indispensable for the electrochemical activation. As shown in Fig. 7, geometry and chemistry of newly developed structure inside ASC would be rather important to evolve the double-layer capacitance effectively. The XRD results shown in Fig. 8 suggest that some ion-insertion process can occur at ASC under highly polarized conditions. However, judging from the shape of the voltammetric responses shown in Fig. 9, we believe that the main contribution to the capacitance evolution, especially in the potential region of 0–1 V vs. Ag QRE, would be based on non-Faradaic process of ion-adsorption/desorption at newly developed active sites. We have found that about 80–90 $F\,g^{-1}$ of specific capacitance could be achieved in every organic solvent electrolyte when proper conditions including the electrolyte composition are chosen for electrochemical activation. The value of the specific capacitance of ASC after the electrochemical activation under the present conditions is still not so high when comparing it with those observed for conventional activated carbons with micropore structures. However, higher operation potential achieved at ASC than conventional activated carbons could be beneficial to be used as a positive electrode of advanced HEC [16].

4. Conclusion

The electrochemical activation of alkali-treated soft carbon (ASC) has been examined in organic electrolyte solutions of various compositions, using potential scanning voltammetry and constant-current polarization methods. The results are summarized as follows.

(1) Both anodic and cathodic polarization induced higher capacitive currents in the following cycles. Its activation behavior also depends on the sort of ions.
(2) In $LiPF_6$ solutions, the activation with anodic polarization was effective for both cation and anion acting as charge compensation species during the charge and discharge of ASC. In $TEABF_4$ solutions, however, the anodic activation only enabled the charge compensation by the anion, and further activation with cathodic polarization was needed for the cation to act as the charge compensation species.
(3) *Ex-situ* XRD patterns of ASC during and after the activation showed that the evolution of active sites for ion adsorption/desorption would accompanied by partly reversible ion-insertion inside the ASC material.
(4) The ASC activated by electrochemical polarization has specific capacitance ranged from 80 to 90 $F\,g^{-1}$ in PC-based and AN-based electrolyte solutions, and showed good rate capability.

Acknowledgement

The authors would like to thank Dr. T. Aida and Mr. I. Murayama, Daihatsu Motor Co. Ltd. for providing samples.

References

[1] R. Kötz, M. Carlen, Electrochim. Acta 45 (2000) 2483.
[2] H. Liu, G. Zhu, J. Power Sources 171 (2007) 1054.
[3] Y. Honda, T. Ono, M. Takeshige, N. Morihara, H. Shiozaki, T. Kitamura, K. Yoshikawa, M. Morita, M. Yamagata, M. Ishikawa, Electrochem. Solid-State Lett. 12 (2009) A45.
[4] M. Ishikawa, M. Morita, M. Ihara, Y. Matsuda, J. Electrochem. Soc. 141 (1994) 1730.
[5] H. Nakagawa, A. Shudo, K. Miura, J. Electrochem. Soc. 147 (2000) 38.
[6] S. Ishimoto, Y. Asakawa, M. Shinya, K. Naoi, J. Electrochem. Soc. 156 (2009) A563.
[7] S. Nomoto, H. Nakata, K. Yoshioka, A. Yoshida, H. Yoneda, J. Power Sources 97 (2001) 807.
[8] P. Simon, A. Burke, Electrochem. Soc. Interface (2008) 38.

[9] S. Nohara, T. Asahina, H. Wada, N. Furukawa, H. Inoue, N. Sugoh, H. Iwasaki, C. Iwakura, J. Power Sources 157 (2006) 605.
[10] E. Frackowiak, V. Khomenko, K. Jurewicz, K. Lota, F. Béguin, J. Power Sources 153 (2006) 413.
[11] T. Aida, K. Yamada, M. Morita, Electrochem. Solid-State Lett. 9 (2006) A534.
[12] M. Takeuchi, K. Koike, T. Maruyama, A. Mogami, M. Okamura, Electrochemistry 66 (1998) 1311.
[13] M. Takeuchi, T. Maruyama, K. Koike, A. Mogami, T. Oyama, H. Kobayashi, Electrochemistry 69 (2001) 487.
[14] S. Mitani, S.-I. Lee, K. Saito, S.-H. Yoon, Y. Korai, I. Mochida, Carbon 43 (2005) 2960.
[15] I.-J. Kim, S. Yang, M.-J. Jeon, S.-I. Moon, H.-S. Kim, Y.-P. Lee, K.-H. An, Y.-H. Lee, J. Power Sources 173 (2007) 621.
[16] T. Aida, I. Murayama, K. Yamada, M. Morita, J. Power Sources 166 (2007) 462.
[17] M. Morita, T. Kaigaishi, N. Yoshimoto, M. Egashira, T. Aida, Electrochem. Solid-State Lett. 9 (2006) A386.
[18] I.-T. Kim, M. Egashira, N. Yoshimoto, M. Morita, Electrochim. Acta 55 (2010) 6632.
[19] I.-T. Kim, M. Egashira, N. Yoshimoto, M. Morita, Electrochim. Acta 56 (2011) 7319.
[20] A.K. Mollner, P.A. Brooksby, J.S. Loring, I. Bako, G. Palinkas, W.R. Fawcett, J. Phys. Chem. A 108 (2004) 3344.
[21] N.G. Tsierkezos, A.I. Philippopoulos, Fluid Phase Equilibria 277 (2009) 20.